10. See, for example, R. E. Ecke, Y. Hu, R. Mainieri, G. Ahlers, *Science* **269**, 1704 (1995); R. V. Cakmur, D. A. Egolf, B. B. Plapp, E. Bodenschatz, *Phys. Rev. Lett.* **79**, 1853 (1997); K. M. S. Bajaj, D. S. Cannell, G. Ahlers, *Phys. Rev. E* **55**, R4869 (1997); H.-W. Xi, X. J. Li, J. D. Gunton, *Phys. Rev. Lett.* **78**, 1046 (1997).
11. P. Marcq, H. Chaté, P. Manneville, *Phys. Rev. Lett.* **77**, 4003 (1996); *Phys. Rev. E* **55**, 3228 (1997).
12. The particular map lattice studied here (Eq. 1) was chosen because of extensive previous work (*15*) uncovering the separation of length scales in the system and because of its symmetry properties. Further work and insight (concerning properties such as the separation of variables into coarse- and fine-grain contributions and the symmetries of the Hamiltonian terms) will be needed to expand the techniques in this report to other popular systems such as a couple lattice of simpler single tent maps.
13. Marcq and co-workers (*11*) have reported that all of the critical exponents of the transition do not agree with the Ising universality class. Rather, some exponents depend on the update rule (for example, Eq. 1a). The results presented here were not tested with the alternate update rule.
14. D. A. Egolf and H. S. Greenside, *Nature* **369**, 129 (1994).
15. C. S. O'Hern, D. A. Egolf, H. S. Greenside, *Phys. Rev. E* **53**, 3374 (1996).
16. L. A. Bunimovich and Y. G. Sinai, *Nonlinearity* **1**, 491 (1988).
17. R. H. Fowler, *Statistical Mechanics: The Theory of the Properties of Matter in Equilibrium* (Cambridge Univ. Press, London, ed. 2, 1955), pp. 659–660.
18. T. Bohr, E. Bosch, W. van de Water, *Nature* **372**, 48 (1994).
19. D. A. Egolf, I. V. Melnikov, E. Bodenschatz, *Phys. Rev. Lett.* **80**, 3228 (1998).
20. D. Durr and H. Spohn, *Nature* **394**, 831 (1998); P. Gespard *et al.*, *Nature* **394**, 865 (1998).
21. Detailed balance and effective Hamiltonians appear for $G \geq 8$. At $G = 8$, finite-size effects are noticeable in the tails of plots such as those in Fig. 3. For $G < 8$, it is not clear whether the breakdown of detailed balance is due to finite-size effects or the non-Gaussian nature of the noise. The requirement $G < \xi_2$ does not appear to be necessary.
22. For values of $\Delta T < 100$, the probabilities of states is still as shown in Fig. 3B; however, the transition rates leading to plots such as Fig. 3A actually appear to give better agreement than expected simply due to the extra crossings as the system wiggles from one state to the next. Temporal coarse-grainings of $\Delta T \geq 100$ create a smoother (less "noisy") transition between states.
23. The 2^{16} states is a small enough number such that a large computational effort yields a large fraction of the states being visited often enough to give statistically significant results. Significantly larger lattices have too many states for meaningful simulations on today's computers. A coarse-grained lattice size of 4×4 is also just large enough such that the dynamics is not overwhelmed by finite-size effects for a wide range of coupling values g.
24. I thank R. Ecke, C. Henley, R. Mainieri, I. Melnikov, and J. Socolar for valuable discussions. This research was supported by the United States Department of Energy under contract W-7405-EN9-36, and the computations were performed on the Nirvana machines of the Advanced Computing Laboratory at Los Alamos National Laboratory and on the Avalon cluster at the Center for Nonlinear Studies.

9 August 1999; accepted 18 November 1999

A Nucleation Site and Mechanism Leading to Epitaxial Growth of Diamond Films

S. T. Lee,* H. Y. Peng, X. T. Zhou, N. Wang, C. S. Lee, I. Bello, Y. Lifshitz†

A diamond nucleation site responsible for epitaxial growth of diamond on silicon by chemical vapor deposition (CVD) is identified in high-resolution transmission electron microscopic images. Other sites in the same sample leading to polycrystalline growth, but deleterious to epitaxial CVD growth, are also described. A mechanism for the heteroepitaxial growth of diamond is suggested, in which etching of the nondiamond carbon binder exposes and removes nonadherent nanodiamond nuclei, leaving intact only those directly nucleated on the silicon substrate. This work enhances our understanding of diamond nucleation and heteroepitaxial growth and its potential applications.

The quest for artificial methods of diamond production is motivated not only by its gemstone quality, but also by its unique set of properties, which make it an excellent candidate for numerous important applications (*1–3*). Diamond was successfully produced in the 1950s by the high-pressure, high-temperature (HPHT) method (*1*, *2*). An alternative method, CVD of diamond at low pressure (typically with the use of an excited CH_4/H_2 mixture on substrates held at ~700° to 800°C), has also been applied successfully over the last 15 to 20 years (*1–3*). The homoepitaxial growth of diamond on a diamond substrate by CVD methods is relatively well understood (*1–3*). Experimental methods for diamond nucleation on nondiamond substrates (the first necessary step of a heteroepitaxial growth process) have also been developed (*4–7*). The most effective method uses bias-enhanced nucleation (BEN) (*4*, *6–10*), in which the target is biased, with a relatively methane-rich CH_4/H_2 mixture (several percent methane) as a first step, followed by a conventional CVD step (typically 1% methane or less). However, the nucleation mechanism of diamond on nondiamond substrates remains poorly understood (*11*), largely because of the tremendous difficulty of locating and identifying the nucleation sites. This is a major obstacle to further advances in diamond science and technology.

Here we present direct high-resolution transmission electron microscopy (HRTEM) evidence that a step on a single crystalline Si surface serves as a nucleation site for heteroepitaxial diamond growth, and we propose a scheme for the growth of epitaxial diamond films on Si wafers.

A BEN treatment with a double-bias–assisted hot filament CVD was used (*12*). In this process, a negative-bias voltage is applied to the Si substrate and a positive-bias voltage is applied to a grid that is placed on top of the hot filament (*13*). The samples were analyzed by HRTEM (*13*), high-resolution scanning electron microscopy (HRSEM), and micro-Raman spectroscopy. Transmission electron microscopy (TEM) observations were made along the [110] direction of the Si substrate.

HRSEM images of the samples show a rough, granular morphology, with an average grain size of about 200 nm. Raman spectroscopy shows a dominant graphitic structure that has no detectable 1330 cm^{-1} diamond peak, but that does have a small peak indicative of "nanodiamond precursors" at ~1100 cm^{-1}. Cross-sectional HRTEM (Fig. 1) shows a grooved Si morphology onto which a predominantly amorphous C (a-C) film is deposited, which explains the Raman data. Diamond crystallites with diameters of about 2 to 6 nm (small enough to identify the nucleation sites) are either embedded in the a-C matrix (white arrows in Fig. 1) or attached to different sites of the Si (black arrows). Selected-area electron diffraction patterns confirmed the diamond structure of the nanocrystallites. No SiC crystallites were found. The diamond crystallites grew randomly (Fig. 2), partially epitaxially (Fig. 3), or perfectly heteroepitaxially (Fig. 4) with respect to the Si surface. In Fig. 3, a set of diamond {111} planes is parallel to the Si {111} planes, which indicates a partially oriented diamond nucleus on Si. The interface between the nucleus and Si near the (001) plane of Si could not be resolved. In Fig. 4, two nuclei have grown epitaxially on stepped areas of the Si substrate. Five to 10 such nuclei have been observed in each of the six samples studied. The diamond crystallites were identified by measuring the spacings of the lattice fringes and the angles of the intersecting lattice planes. This measurement is very precise because the Si (111) lattice in the same image can be used as an internal reference. In Fig. 4A, the interfaces between the diamond crystallite

Department of Physics and Materials Science and Center of Super-Diamond and Advanced Films, City University of Hong Kong, Hong Kong, China.

*To whom correspondence should be addressed. E-mail: apannale@cityu.edu.hk

†On leave from Soreq Nuclear Research Center, Yavne 81800, Israel.

(~2 nm) and the Si substrate are $(1\bar{1}1)$ and $(\bar{1}11)$ for both diamond and Si crystals, intersecting at an angle of 109.5° (Fig. 4A). The $(1\bar{1}1)$ plane of the diamond crystallite deviates by about 1° to 2° from the $(1\bar{1}1)$ plane of the Si crystal. This deviation may be due to the small size of the diamond crystallites and the large mismatch between the lattice parameters of diamond and Si. In contrast, the diamond crystallite that nucleates on the {111}-{001} intersecting steps of the Si substrate shows perfect epitaxial orientation (Fig. 4B). A Fourier transform of this sample (inset in Fig. 4B) confirms the diamond nature of the [110]-oriented crystallite and the epitaxial relation between the diamond nucleus and the Si substrate. No misorientation between the crystallite and the Si substrate was detected, which shows that the epitaxial diamond crystallite is grown directly on the stepped {111} and {001} surfaces of the Si substrate.

We propose that both nucleation sites in Fig. 4 contribute to the epitaxial growth of diamond on Si. The direct observation of these small diamond crystallites enables the reliable determination of the location of the nucleation site, which seems to be the Si step. Even for a high nucleation site density, say $10^{10}/cm^2$, it would be very difficult to locate the original nuclei (one 2- to 6-nm-diameter crystallite per 100 nm by 100 nm). This explains why previous studies, to the best of our knowledge, have failed to locate such a nucleation site. Moreover, the probability of simultaneously observing by HRTEM two different interfaces between the diamond nucleus and the Si substrate is still smaller than the probability of observing the diamond nucleus itself. The poor epitaxial quality of the crystallite in Fig. 4A compared with that in Fig. 4B may be related to the different growth planes [(111) compared with (001), respectively]. Thus a step appears to be needed for nucleation, but the epitaxial quality may be dependent on the Si planes on which the diamond is grown.

We propose a sequence of events that should lead to a heteroepitaxial growth of diamond films. On the basis of the above observations and on previously reported processes, BEN results in the formation of a variety of different nucleation sites, some that are related to the Si substrate and some that are located in the C matrix, which is an inhomogeneous composite of C structures. Because the subsequent CVD growth process is characterized by a smaller CH_4/H_2 ratio than the BEN process, the nondiamond C matrix should be chemically etched by atomic hydrogen. This etching would produce a dust of diamond particles, which would probably not adhere to the surface, in contrast to the diamond crystallites nucleated on Si steps, which should adhere. The quality of the heteroepitaxial growth of diamond on Si after BEN would thus be dependent on the relative number of epitaxial nucleation sites on the Si. The Si substrate is a single crystal, and diamond growth on all the aligned nucleation sites located on Si (that is, the steps) should therefore lead to the coalescence of the crystals as experimentally observed with BEN. The growth of crystallites of exactly the same orientation is a constructive process, as far as the coalescence of these crystallites is concerned, but is a destructive process for the growth of other orientations, which leads

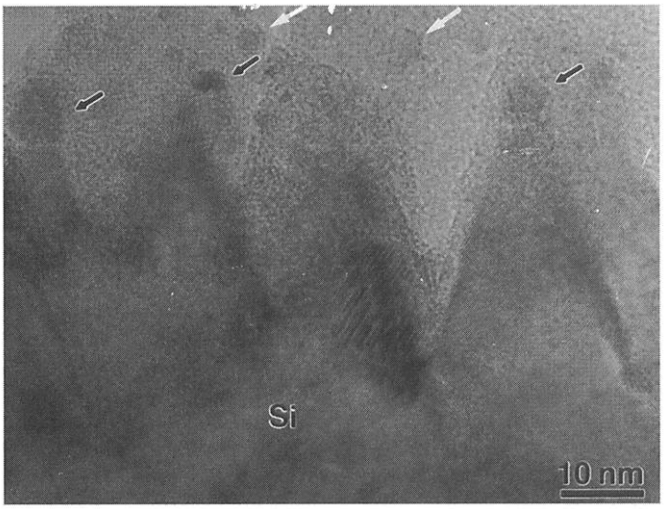

Fig. 1. A low-magnification planar view of the interface between the Si substrate and the C film indicates small (2 to 6 nm in diameter), randomly dispersed diamond crystallites. Some have grown on the Si (black arrows) and some are embedded in the a-C matrix (white arrows). Neither a SiC layer nor SiC crystallites are present.

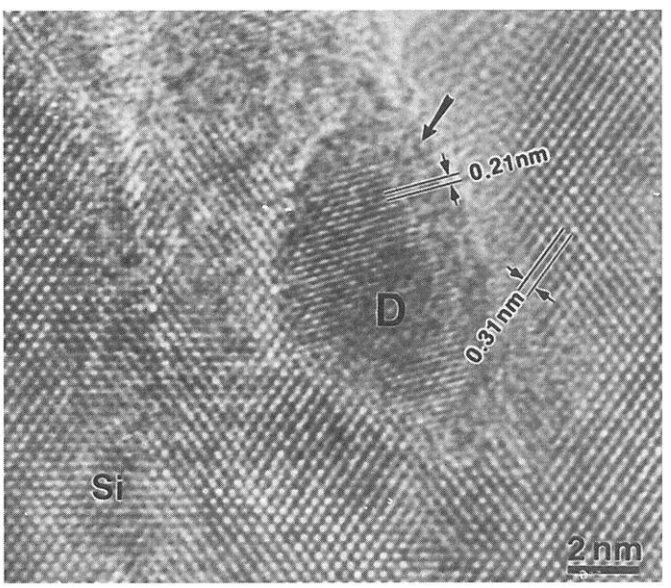

Fig. 2. HRTEM image of a diamond crystallite (diameter ~6 nm) grown directly on Si with a random alignment.

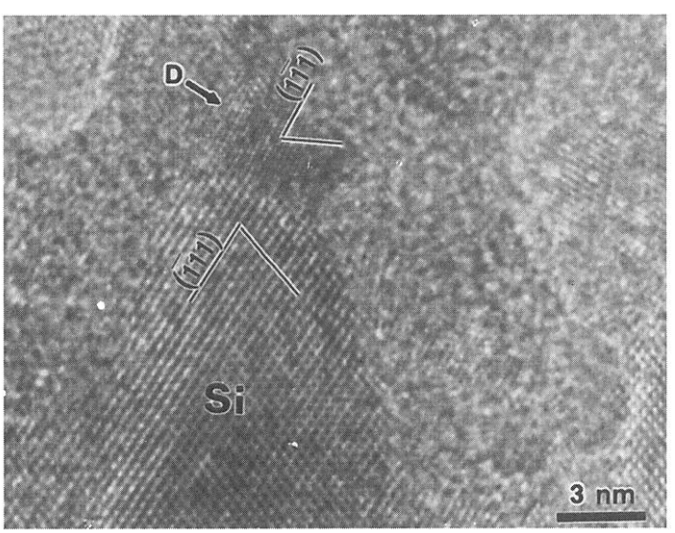

Fig. 3. HRTEM image of a diamond crystallite (diameter ~3 nm) grown directly on Si with a partially epitaxial alignment.

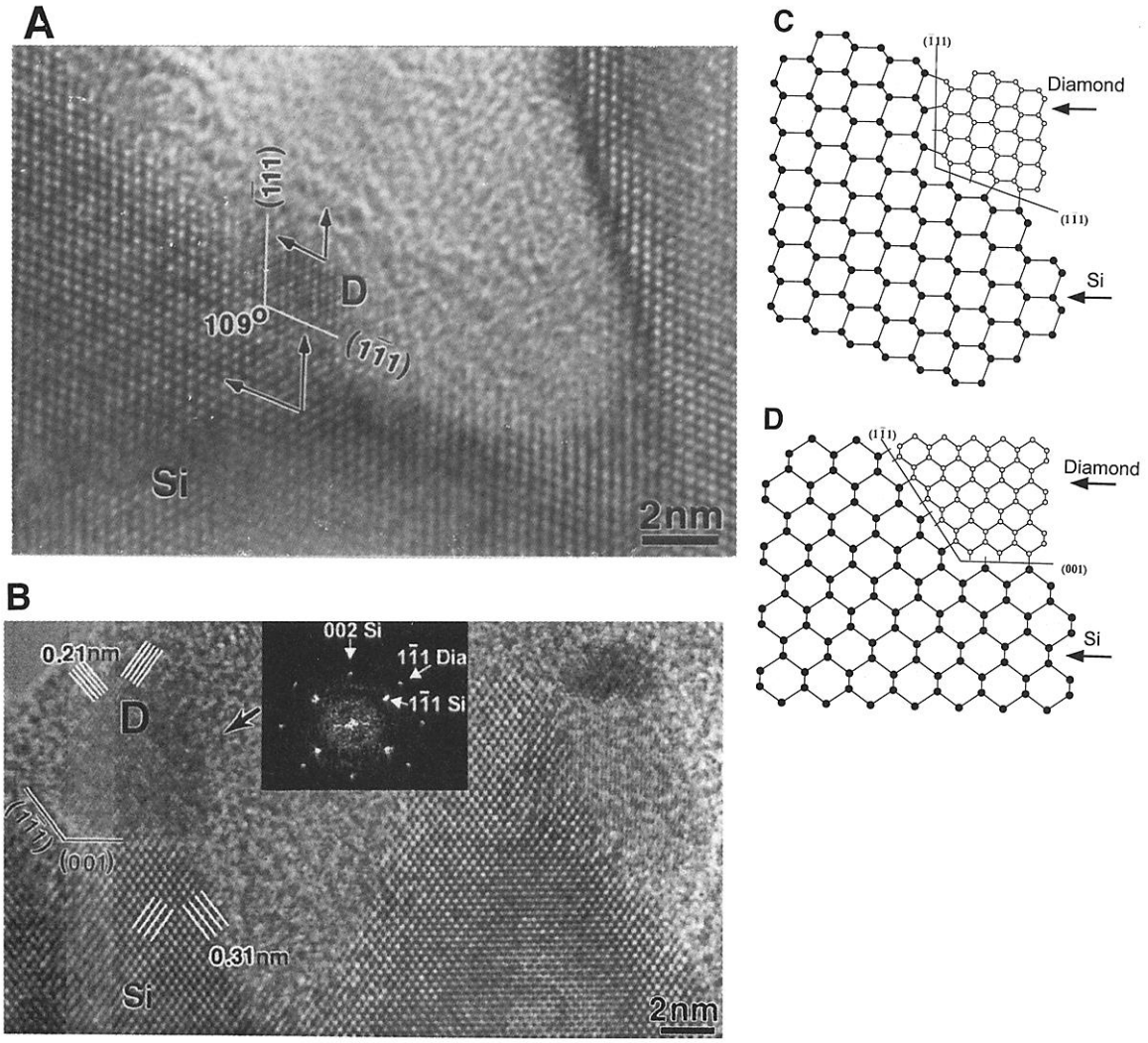

Fig. 4. (**A**) HRTEM image of a diamond crystallite (diameter ~2 nm) grown directly on a Si step with an epitaxial alignment. The interfaces between the Si and the diamond are $(\bar{1}11)$ and $(1\bar{1}1)$, intersecting at an angle of 109.5°. (**B**) HRTEM image of a diamond crystallite (diameter ~6 nm) grown directly on a Si (001) surface with an epitaxial alignment. No misorientation between the diamond nucleus and the Si substrate was detected. (Inset) The Fourier transform of the diamond crystallite and the interatomic spacings confirm the diamond nature of the crystallite. (**C** and **D**) Ball-and-stick diagrams illustrate the interfaces between the diamond crystallites and the Si substrate in (A) and (B).

to their suppression. This selective growth effect is enhanced when deposition conditions for which the diamond growth rate is larger in specific directions are chosen (*14*). The effect of other (nonaligned) sites would be the deterioration of the epitaxial quality of the CVD diamond. Thus the way to achieve a better heteroepitaxy should be to increase the number of epitaxial nuclei with respect to others in the nucleation stage, and then to enhance the elimination of others in the growth stage.

A variety of previous works addressed the diamond nucleation mechanism, especially when using BEN. The suggested mechanisms include (i) subplantation of C-containing species into subsurface sites to form a stress-induced sp^3 cluster, which serves as a precursor to the diamond nucleus formation (*4*); (ii) nucleation of diamond on steps of graphitic planes formed by the BEN process (*10, 15*); (iii) formation of diamond nuclei in an epitaxial SiC layer deposited on Si (*8*); and (iv) induction of plasma chemistry changes by biasing (*6*). The nucleation of a diamond crystallite on the specific Si step identified here could be a result of a "mold effect," that is, the boundary conditions imposed by at least two Si surfaces on the evolution of the C phase, as suggested by Lifshitz *et al.* (*16*). This study is also relevant to other debated issues in diamond nucleation. One is the critical size of the diamond nuclei, which is found to be less than ~2 nm (the smallest crystalline size detected by us). Another issue is the role of SiC in diamond nucleation (*8*). Like a Si nucleation site, a SiC site may deliver the necessary information on the Si registry to the diamond nuclei, starting with an epitaxial growth of SiC on Si and followed by the epitaxial growth of diamond on SiC. No SiC crystallites were detected here, which indicates that their existence is not vital for the nucleation process. Nevertheless, this does not exclude the role of SiC in other deposition schemes.

References and Notes

1. J. C. Angus and C. C. Hayman, *Science* **241**, 913 (1988).
2. A. Paoletti and A. Tucciarone, Eds., *The Physics of Diamond: International School of Physics, "Enrico Fermi" Course 135*, (IOS Press, Amsterdam, 1997).
3. Diamond Films: Recent Developments, D. M. Gruen and I. Buckley-Golder, Eds., *Mater. Res. Soc. Bull.* **23** (no. 9) (1998).
4. S. Yugo, T. Kania, T. Kimura, T. Muto, *Appl. Phys. Lett.* **58**, 1036 (1991).
5. A. A. Morish and P. E. Pehrsson, *Appl. Phys. Lett.* **59**, 417 (1991).
6. B. R. Stoner, G.-H. Ma, S. D. Wolter, J. T. Glass, *Phys. Rev. B* **45**, 11067 (1992).
7. X. Jiang, W. J. Zhang, C. P. Klages, *Phys. Rev. B* **58**, 7064 (1998).
8. R. Stockel *et al.*, *J. Appl. Phys.* **83**, 531 (1998).
9. S. Yugo, N. Nakamura, T. Kimura, *Diamond Relat. Mater.* **7**, 1017 (1998).
10. J. Gerber *et al.*, *J. Appl. Phys.* **79**, 4388 (1996).
11. J. Butler and H. Windischmann, *Mater. Res. Soc. Bull.* **23**, 22 (1998).
12. X. T. Zhou *et al.*, *Diamond Relat. Mater.*, in press.
13. The BEN conditions were as follows: CH_4 concentration of 3.5%, a filament temperature of 2100°C, a substrate temperature of 850°C, a pressure of 30 torr, a grid voltage of 28 V, and a substrate voltage of −150 V. The BEN treatment duration was 0.5 hours, and the substrate current density was 3 mA/cm^2 (that is, an estimated ion dose of 3×10^{19} ions per square centimeter). HRTEM was done on a Phillips CM200 FEG TEM at 200 keV. The TEM samples were prepared by mechanical polishing followed by Ar ion milling.
14. H. Kawarada, in (*2*), p. 505.
15. W. R. Lambrecht *et al.*, *Nature* **364**, 607 (1993).
16. Y. Lifshitz, S. R. Kasi, J. W. Rabalais, *Phys. Rev. Lett.* **62**, 1290 (1989).

17. Supported in part by the Research Grants Council of Hong Kong (no. 9040343) and the Strategic Research Grants of the City University of Hong Kong.

19 July 1999; accepted 16 November 1999